ADVANCED STRUCTURAL ASSESSMENT TECHNIQUES OF CAST IRON RAILWAY ARCH BRIDGE

Ł. Zymla[1], W. Zielichowski-Haber[2], M. Majka[3]

[1]Zymla Consulting Ltd., York, UNITED KINGDOM.
[2]Mouchel, York, UNITED KINGDOM.
[3]ASECon (Advanced Structural Engineering Consultants), POLAND.

e-mails: lp.zymla@gmail.com, w.zielichowskihaber@gmail.com, mm@asecon.pl

SUMMARY

This paper discusses an approach towards an advanced structural assessment of a listed cast-iron arch bridge. The bridge used as a case study is a two-span structure located in the North of England and carrying two railway tracks over the River Calder. The structural assessment has been carried out using advanced numerical methods as part of the ongoing effort to maintain and enhance the lifespan of the structure.

Keywords: *Railway, arch bridge, LUSAS, non-linear, analysis, assessment, 3D model.*

1. INTRODUCTION

Cast iron structures became popular in the early 19th century. Bridge spans of up to 15m were mainly built using cast iron primary beams supporting jack arches or transverse iron or timber decks. For larger spans cast iron arches in two or more sections bolted together and restrained with wrought-iron or cast iron ties were popular until about 1847 [1]. Many short span road bridges with cast iron girders and brickwork jack arches, particularly over waterways and railways, are still in use.

Following the Dee Bridge failure in 1847, it was found that some railway engineers had used factors of safety as low as 3. That was considered exceptionally low for rail structures as such factors were typical for cast iron beams in buildings and the subsequent increase in engine weight from 12 to 30 tonnes effectively reduced the safety factor of some structures to approximately 1.0. Consequently, a factor of safety of 6 for railway structures was typically recommended [1]. The use of simply supported cast iron beams with transverse jack arches or metal or timber floors continued to be regarded as a safe and economical solution. Most engineers appear to have taken the view that it was the structural form rather than material that failed.

Some of the 19th century design theories, particularly Tredgold's safe working load method, assumed high tensile strengths and this resulted in factors of safety of slightly above 1.0 for large beams. From around 1900, Clark's exact solution using stress—strain curves from compressive and tensile tests indicated that the assumption of completely elastic behaviour theoretically resulted in underestimates of up to 30% in the strength of cast iron beam capacities. However, the exact solution method yielded discrepancies in capacity when compared with tests that varied with the physical shape of the beams and became known as the shape factor [1].

Until about 1830 iron was smelted using coke as a fuel with steam engines blasting cold air into the furnaces. The melted iron was poured directly into moulds. Around the 1830s the technology evolved to use heated up blast air which improved the economy and productivity and enabled coal to be used instead of coke directly in the furnace. This in turn increased production of hot blast iron that became widely popular after 1830.

The properties of cast iron varied considerably before 1830 but the use of coal introduced impurities that further varied the properties of the product. In Metallurgical terms, cast iron is a corrosion resistant, brittle alloy with about 2.5-4% carbon content and mechanical properties highly sensitive to the cooling process. A relatively slow rate of cooling in the mould leads to the formation of grey cast iron in which the carbon solidifies into graphite flakes surrounded by a metal alloy with steel-like properties. A rapid rate of cooling ensures that the carbon has no time to solidify and is instead combined with the iron producing fine grained, stronger, harder and more brittle white cast iron. Other impurities are silica and phosphorus for grey cast iron and sulphur for white cast iron as well as slag from the furnace. The stress-strain relationship varies considerably according to chemical composition and manufacturing process. The material is highly anisotropic with poor tension and shear performance but it performs well in compression with nearly elastic behaviour. Another significant variable in the properties of cast iron is the form factor - the cooling rate characterised by volume to surface area ratio. This results in rapid cooling for small and uniform cross sections giving stronger but more brittle material. For larger cross sections the ratio dictates the rate at which different parts are cooling causing the material at the centre to appear porous. As a result the probability of weak spots intensifies considerably. The resulting tensile strength difference between small and large section can be as much as 300%.

In the 19th century there was very little quality control or material specification in place in comparison to current manufacturing. The iron founders and engineers each had a favoured recipe of different types of pig-irons for a particular type of casting with quality of metal judged by tests performed on small bars made from the same melt. The moulding was in clayey sand material and slightly oversized to allow for shrinkage and cooling. The beams were to remain in the casting for cooling but it was not uncommon in small foundries to remove beams whilst they were red hot to accelerate production and this led to numerous defects. A common flaw being a blow-hole where gas bubbles and slag become trapped beneath the surface causing a structural flaw or solidification of the metal from the cold surface of the mould towards the centre of the section causing voids to form often at flange to web junction.

2. DESCRIPTION OF STRUCTURE & INFORMATION USED IN THE ASSESSMENT

The railway bridge presented in this article is a two span example of a listed cast iron structure constructed circa 1847 and situated on the West Coast Main Line where it crosses river Calder on the Thornhill LNW to Whitehall West Jn. route. Each span comprises six longitudinally spanning segmented cast iron arches (five segments bolted together in each arch) interconnected by cast iron cross bracing and transverse wrought iron tie rods assembled using a socket and wedge technique. Each outer segment has a top chord and bottom rib connected by decorative vertical cast iron spandrel elements, the central segment merging the arch rib and top chord. The arches support a deck comprising transversely spanning modern steel troughing filled with lightweight concrete which in turn supports the ballasted permanent way and decorative cast iron parapets. Each span is approximately 9.750 m wide measured square between the

parapet edges. Both spans have a clear span of 30.785 m (101') with an approximately 37° skew. The structure carries two tracks with a linespeed of 75 mph and is supported by two outer end abutments and an intermediate masonry pier. The overall length of the structure including wing-walls is approximately 84.2m. The foundation details are not known but the substructure shows no sign of visible distress.

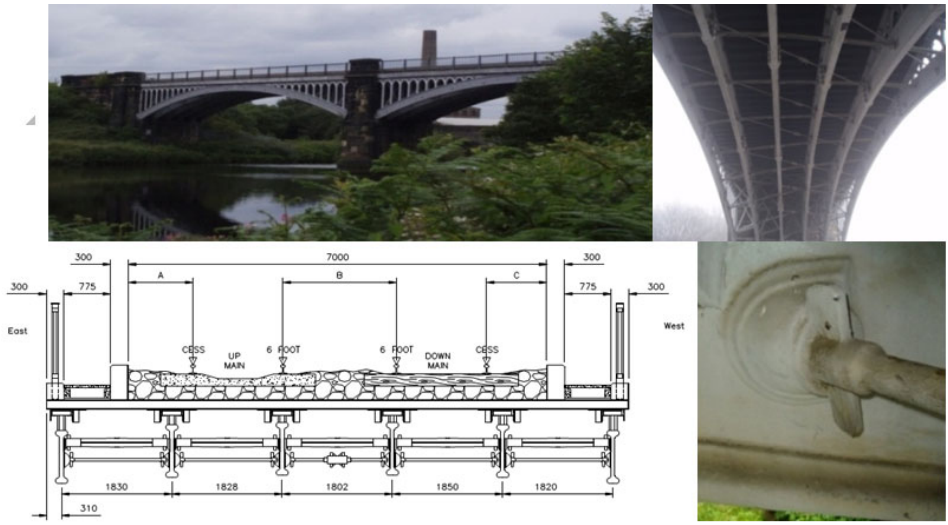

Fig. 1. *Elevation, section and connection details.*

3. NUMERICAL ASSESSMENT

The assessment was undertaken to establish the theoretical capacity of the structure. Initially a single arch rib was idealised using 2D frame model with pinned supports and spandrel posts modelled as pin-joined (Fig. 2). Simplified calculation of dynamic response of the structure was carried out based on the Network Rail NR/GN/CIV/025 Assessment Code.

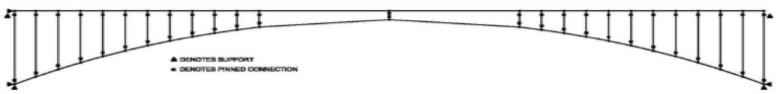

Fig. 2. *2D model.*

The live load has been calculated using the RA1 type Network Rail standard vehicle (Fig. 7) with the axle loads positioned to obtain the worst load effects in the arch rib. The transverse distribution of load from the track to the arches below was carried out using simple static. The dynamic factor calculated assuming the determinant length for dynamic amplification factor for arches $L\phi = 0.5L$ was: bending - 1.68 at 75 mph; fatigue - 1.216 at 75 mph.

The combined bending and axial interaction calculations carried out using the Gordon-Rankine formula for axial buckling combined with Network Rail's theoretical cast iron buckling curves indicated that the structure has zero live load capacity at the current line speed.

An advanced model was proposed to further investigate the behaviour of the structure. The bridge was 3D laser scanned and the information used as the input geometry in LUSAS Finite Elements Analysis package. The dynamic and buckling response of the bridge was investigated ignoring any defect detected. During the analysis it became evident that the structure represented a significantly distorted version of the idealised 2D model with vertical and horizontal eccentricities in excess of 150mm and the main arch ribs distorted (twisted) and vertically leaning to one side. Due to the size of the central pier, it was considered that the superstructure could be accurately represented by a single span model. Therefore, the model incorporated six main cast iron arch ribs, wrought iron tie bars and cast iron cross-bracings of a single span only (Fig. 3).

The following assessment methodology was proposed: Stage 1 – elastic model to verify the initial stresses and investigate the load distribution; Stage 2 – elastic buckling analysis (Eigenvalue) to predict the buckling behaviour of the structure; Stage 3 – dynamic analysis - natural frequency check to predict the dynamic response of the structure; Stage 4 – check of fatigue stresses for critical load case.

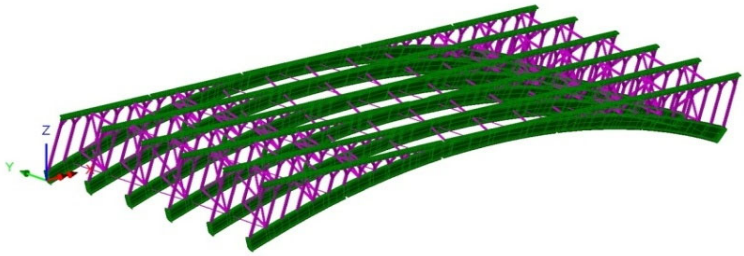

Fig. 3. *LUSAS model.*

The main arch ribs, top chords, rib connections and end plates at the supports were modelled as thick shell surface elements. Shell eccentricities were applied into the LUSAS model to take account of the eccentricity of the elements from their nodal positions and to minimise duplication of the stiffness in the nodes (Fig. 5).The transverse struts, ties and frames between the arch ribs were modelled as thick beam elements.

3.1. Support conditions

The support conditions at the ends of the arch ribs and spandrel top chords are critical in determining the true response of this structure to live load. The cast iron arch ribs bear normally onto bearing plates inclined to the substructures with a combination of bearing plate, side edge strips and masonry/ cast iron friction force between the abutting faces providing the vertical and horizontal restraint. There are no holding down bolts visible to restrain any possible lift off effects. The top chords appear to be inserted into the masonry abutment to an unknown depth and there is no record of the bearing arrangement for these (Fig. 6).

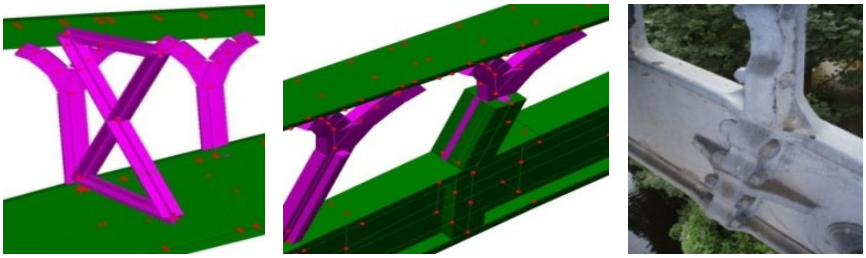

Fig. 5. *Detail showing internal rib with connection plates and bracings.*

If both the top chords and arch ribs were considered to be fully fixed at the supports and the overall rib and spandrel structure considered to be suitably stiff, the behaviour would tend to be that of an end restrained beam governed by the combined hog bending and shear capacity at the supports and the sag bending at mid span. In terms of deflection, it would be likely to result in a full span critical mode shape and thus a full span determinant length for dynamic analysis. If the top chord is unrestrained it may be that the structural action resorts to that of a conventional arch resulting in a half span determinate length giving a greater dynamic increment (as assumed in initial calculations where $L\phi = 0.5L$).

Fig. 6. *Main Arch Rib end support & Top Chord end support (External Rib).*

In order to test the sensitivity of the structural response to the support conditions five models were created and analysed.

- Model 1 – a single point pinned support at each rib's end plate (XYZ fixed for translation). Transverse line support at each top chord (DY fixed).
- Model 2 – two line support at each rib's end plate (XYZ fixed for translation) effectively giving a form of moment connection. Transverse line support at each top chord (DY fixed).
- Model 3 – as model 1 but top chords additionally fixed longitudinally using single point support (DX fixed).
- Model 4 – as model 2 but top chords additionally fixed longitudinally using single point support (DX fixed).

- Model 5 – supports arrangement as per model 4 but with spring supports applied. The spring stiffness calculated to allow for an average 5mm displacement of the rib's end plate at the spring location under full RA1 vehicle load. Additionally, 1/3 of the spring stiffness value applied to the top chord in DY and DX direction.

Material properties: the material properties were defined as below:

Cast Iron:	Wrought Iron (ties):
E = 114.0E3 N/mm^2	E = 190.0E3 N/mm^2
Poisson's ratio = 0.25	Poisson's ratio = 0.3
Density = 7.2E-9 t/mm^3	Density = 7.7E-9 t/mm^3

3.2. Application of load in the model

Cast iron and wrought iron self-weight is applied directly in LUSAS as gravity (body) force. Troughing, concrete, ballast, track loading and Live loading due to Type RA1 vehicle is applied as a UDL load to the top of the chord. For the frequency check, only permanent load plus a 10kN point load is applied as per NR/GN/CIV/025.

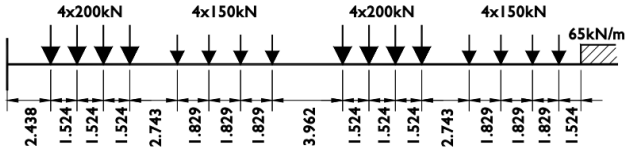

Fig. 7. *20 BSU RA1 Type of Loading (RA10).*

3.3. Boundary conditions and assumptions made

The medium E value is used for cast iron as recommended by Network Rail assessment code. The material is assumed to be of good quality i.e. no variation in E values, density, no hidden defects and weak spots, no variation in stress-strain characteristic or Poisson's ratio. The sensitivity of structural response to the variation in stiffness i.e. variation in E value distribution can be ignored.

As the buckling failure of the main ribs is due to combined axial buckling and lateral torsional buckling failure, there is no simple way of calculating the corresponding effective buckling length. Each of those buckling failures are covered separately by the Assessment Standard with no common approach towards buckling length. Therefore the failure criteria for elastic buckling has been arbitrary chosen to be global factor of safety of 5.0 in accordance with the historical Gordon-Rankine formula and is assumed to account for casting impurities and material brittleness.

The limiting capacity for fatigue is defined as onset of permissible fatigue stress limit reached for two adjacent Gauss Points across the width of a single FE or adjacent FE (i.e., approaching material rupture at fatigue stress state).

4. RESULTS

Load distribution: A comparison between simplified hand calculations and the 3D load distribution carried out for all five models revealed a maximum 7% increase in the load on the critical arch rib, reduced to zero when spring support conditions were considered (Model 5). A summary of the distribution results is given in Table 1 below. Using a 3D model for enhanced load distribution for this type of structure is therefore of no significant benefit.

Table 1. *Comparison between resultant support reaction (Static)for the worst loaded Rib 4.*

Distribution model	Rib 4 Resultant	Difference with Level 1
Level 1	2903kN	N/A
Level 1A - Model 1	3082kN	6%
Level 1A - Model 2	2953kN	2%
Level 1A - Model 3	3111kN	7%
Level 1A - Model 5	2906kN	0

5. LINEAR BUCKLING ANALYSIS

A linear analysis may be applied to relatively 'stiff' structures to estimate the maximum load that can be supported prior to structural instability or collapse. In LUSAS the buckling prediction is obtained using an Eigenvalue method where the Eigenvalue is one of the particular values of a certain parameter for which a differential equation or matrix equation has an Eigen function. The buckling analysis was carried out for Model 1 only because of the incompatibility of the spring support cases in converging solution. The analysis returned diagonal decay warnings associated with poor conditioning of the stiffness matrix due to the relative low stiffness of the listed structure. A linear buckling analysis uses a single load case and as such with the dead + superimposed dead + live load (DL+SIDL+LL) (RA10 nominal static) loadings being combined. The theoretical Load Factor is a multiplier of the applied load. Buckling load factors obtained were first calculated with 1.0xRA10 (nominal static) and then recalculated with DL+SIDL+5.0xRA10 static loading to establish the sensitivity of the live load multiplier on the buckling factor. It was found that the sensitivity of results is about 10% when compared with the case of DL+SIDL+1.0xRA10. The relatively good correlation of the result allows an approximate dynamic buckling load factor to be calculated directly from the static load case. The minimum buckling load factor is presented in Table 2. It can be seen (Fig.8) that the critical mode of response is associated with the full loaded length of the span which is associated with the quasi torsional restrains provided by the intermediate transverse restraints.

Table 2. *Elastic buckling load factor as a multiplier of dead, superimposed and live loads.*

	Load Case 3
Load F. (DL+SIDL+RA 8 static)	3.59
Load F. (DL+SIDL+RA 8 dynamic)	2.79

As demonstrated, a minimum load factor of 2.79 would need to be considered for the applied loads (DL + SIDL + LL (RA8 Nominal Dynamic)) in order to cause buckling of the Cast Iron ribs and this would indicate that there is tendency towards buckling under assessment loads if account is taken of possible material and casting deficiencies (the original factor of safety of 5 in Gordon-Rankine formula is assumed to cover that).

Fig. 8. *Model 1 Eigenvalue 1. RA10 (ribs only).*

5.1. Dynamic Analysis

The pinned arch rib end assumption (as for the simplified analysis) - as opposed to moment transmitting rib end assumption - tends to increase the dynamic factor by up to 9% for the first fundamental mode, but only up to 3.5% for the second fundamental mode. The pinned and fully restrained (in plane) top chord end assumption (as for the simplified analysis) - as opposed to the longitudinally free end assumption - makes virtually no difference to either the first or second fundamental modes. The determinate length is the full span for the first fundamental mode and half span for the second fundamental mode, with the largest change in lateral displacements occurring in the top chords near the ends. When the top chords were assumed to be fully unrestrained longitudinally a movement of only 1.9mm to 2.78mm occurred under application of DL+SIDL+1.0LxRA10 (dynamic). This deflection is of a realistic magnitude and therefore it is not considered reasonable to assume that the abutments offer any longitudinal restraint to the top chord / stringer beams (as models 3 & 4) that can be guaranteed. Even with some intermediate assumptions regarding the interaction between superstructure and substructure (modelled as spring supports in Model 5) the increase in the dynamic factor against the fully fixed arch rib end case (Model 2) is of the order of 4% percent for strength and 2.3% for fatigue for the first mode, and 1.3% for strength and 1.4% for fatigue for the second mode. There is a significant difference between natural frequencies obtained using 2D and 3D models. This is due to the fact that the 2D simplified method used midspan deflection and the natural frequency formula for a simply supported beam to estimate dynamic effects (as per the Assessment Code).

Table 3. *1st and 2nd fundamental mode of response where Lϕ determinant length, No natural frequency, DF dynamic factor.*

Model	First Fundamental Mode (Eigenvalue 1)				Second Fundamental Mode (Eigenvalue 2)			
	Lϕ [m]	No[Hz]	DF (Bndg)	DFr (Ftg)	Lϕ [m]	No[Hz]	DF (Bndg)	DF (Ftg)
2D	L	6.76	1.154	1.060				
FE 1	1.0L	1.71	1.445	1.226	0.5L	3.096	1.636	1.291
FE 2	1.0L	2.16	1.327	1.165	0.5L	3.625	1.587	1.253
FE 3	1.0L	1.72	1.439	1.223	0.5L	3.116	1.634	1.290
FE 4	1.0L	2.17	1.325	1.165	0.5L	3.632	1.631	1.289
FE 5	1.0L	1.93	1.378	1.192	0.5L	3.352	1.607	1.270

The results show that the structure's response is relatively insensitive to the variation in support condition with the first mode of natural frequency represented by lateral displacement with a half wavelength equal to the span, and with the second mode of response as an asymmetrical displacement with half wavelength equal to half of the span. It could be argued that the first mode of response corresponds with beam-like behaviour with a small vertical normalised displacement and the second is clearly asymmetric both vertically and horizontally with a higher normalised vertical displacement thus representative of arch type behaviour. It is therefore considered prudent to assume that the critical mode of response is that associated with an arch, resulting in a dynamic factor of 1.607 for strength and 1.27 for fatigue based on the flexible spring ended restraint (Model 5) results (Fig. 9).

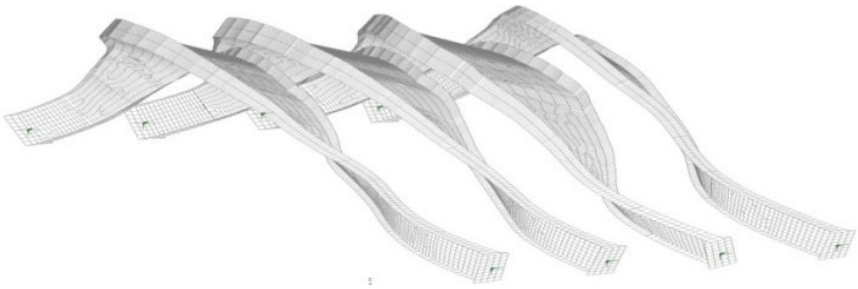

Fig. 9. *Model 5 Eigenvalue 2 (4 internal ribs only).*

5.2. Elastic Stress Check

The permissible fatigue stress in cast iron depends on the proportion of dead load stress in the section. To calculate the total allowable fatigue stress limit, the dead load effects must first be separated and included in the fatigue calculations. The fatigue safe stress model in historic cast iron is non-linear [2]. The stress check revealed overstress in the posts to rib connection under certain load arrangements with the tensile stresses above allowable for both fatigue and working stress limit. The stress concentration at that location results in localised failure of the top flange to post connection and could lead to theoretical progressive failures of the posts as loads redistribute, with accompanying loss of restraint to the ribs and eventual collapse. Such cracked posts have been identified during inspection showing good correlation with the model's prediction (Fig. 10).

Fig. 10. *Crack in vertical posts, ribs connections and bracing to ribs connection.*

6. CONCLUSION

The structure has been modelled in 'as-built' condition without taking into account the numerous defects recorded during inspection for assessment. There is evidence of blow holes, linear casting defects and cracks to the main elements. The elastic buckling analysis indicates a relatively modest buckling load factor which suggests that the structure is susceptible to buckling failure. Numerous problems with the buckling analysis attributed to the general lack of stiffness in the modelled structure and quasi-torsional restraint to the main ribs provided by the bracing system suggests that the use of FEM analysis for such type of structure should be approached with caution. The date of construction suggest that is has been designed with a low overall safety factor, with a safety margin on tensile effects in the larger members less than expected due to shape factor. The structural problems only became evident when the heavy goods traffic started using this route. The stress analysis revealed significant stress concentration in the spandrel to rib connection with some localised fatigue stress concentration in the main ribs. A number of connections were found to fail on site leading to the conclusion that there is ongoing progressive damage occurring to the structure. The risks of hidden defects (cold joints, foundry dirt, mould sand, slag and other inclusions, blow holes, local stress raisers at features, residual stresses from differential cooling plus material variation from the same) are considerable. The signs of distress evident and the time delay associated with the risk of progressing any further testing and research into the material properties and not getting a sufficient improvement in capacity means that there is an unacceptable risk of Network Rail having to close the line to traffic if the signs of distress progress before any strengthening solution could be implemented. In light of the above, an intervention is recommended and the proposal is to construct a new simply supported structure concealed within the existing cast iron elements. The scheme is currently being developed.

The authors would like to thank Network Rail Assessment Team in York (London North East) for their contribution to the paper.

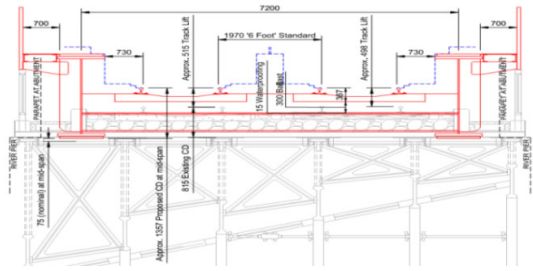

Fig. 14. *Intervention.*

REFERENCES

[1] SWAILES T., *19th century cast iron beams. Their design, manufacture and reliability*, Proceedings of Institution of Civil Engineers, Civil Engineering, February 1995, (25-34).

[2] Network Rail, Assessment of Underbridges (Network Rail assessment code), *Civil Engineering*, NR/GN/CIV/025 Issue 3, 2006, (Section 9, 1-7).